Acta Cryst E CRYSTALLOGRAPHIC COMMUNICATIONS

ISSN 2056-9890

Crystal structure and Hirshfeld surface analysis of chiral *catena*-poly[L-histidinediium [[diiodidocuprate(I)]-μ-iodido] monohydrate]

Valerii Y. Sirenko,[a]* Valeriia N. Ovdenko,[a] Vadim A. Potaskalov,[b] Mircea-Odin Apostu[c] and Il'ya A. Gural'skiy[a]

[a]Department of Chemistry, Taras Shevchenko National University of Kyiv, Volodymyrska St. 64/13, Kyiv 01601, Ukraine, [b]Department of General and Inorganic Chemistry, National Technical University of Ukraine "Igor Sikorsky Kyiv Polytechnic Institute", Beresteiskyi Pr. 37, 03056 Kyiv, Ukraine, and [c]Department of Chemistry, Faculty of Chemistry, Al. I. Cuza University of Iasi, Carol I Blvd. 11, Iasi 700506, Romania. *Correspondence e-mail: valerii_sirenko@knu.ua

Received 20 October 2025
Accepted 10 November 2025

Edited by S.-L. Zheng, Harvard University, USA

Keywords: crystal structure; distortion indices; L-histidine; chirality; helical; Hirshfeld surface analysis; materials; one-dimensional halides; copper(I); amino acids; iodides; A_2CuX_3-type compounds.

CCDC reference: 2501923

Supporting information: this article has supporting information at journals.iucr.org/e

The title compound, $\{(C_6H_{11}N_3O_2)[CuI_3]\cdot H_2O\}_n$ or (L-HisH$_2$)CuI$_3$·H$_2$O (**1**), is a chiral organic–inorganic compound that crystallizes in the monoclinic $P2_1$ space group. The asymmetric unit of **1** consists of one diprotonated L-histidinium cation {4-[(2*S*)-2-azaniumyl-2-carboxyethyl]-1*H*-imidazol-3-ium}, one Cu^+ cation, three iodide anions, and one co-crystallized water molecule. The Cu^+ cations is four-coordinated by iodide anions forming a [CuI$_4$] unit. Structural analysis of the [CuI$_4$] unit using the Baur, τ_4, and τ_4' indices reveals its slight deviation from ideal tetrahedral geometry. Two iodide anions from each [CuI$_4$] unit bridge adjacent Cu^+ centers, forming chiral left-handed helical $[CuI_3]_n^{2n-}$ polymeric chains. The biprotonated L-histidinium cations balance their negative charge and form N—H···I, O—H···I, and weak C—H···I hydrogen bonds with the $[CuI_3]_n^{2n-}$ chains. According to the Hirshfeld surface analysis, the main contributions to the crystal packing arise from H···I and H···O contacts, while C···I and N···I interactions indicate the presence of I···π contacts. The compound reported here represents the first example of a chiral A_2CuX_3-type metal halide, which shows potential for second-harmonic generation, polarized blue-light emission, and other non-linear optical applications.

1. Chemical context

Recently, copper(I) halide materials have attracted significant interest because of their promising properties for applications in optoelectronics and radiation scintillators (Popy *et al.*, 2024; Kirakci *et al.*, 2017; Banerjee & Saparov, 2023; Chen *et al.*, 2025; Du *et al.*, 2023; Zhang *et al.*, 2024). Copper(I) halide-based materials exhibit high photoluminescence quantum yields, tunable crystal structures, and, thanks to their structural and chemical diversity, feature adjustable band gaps and photophysical properties (Banerjee & Saparov, 2023). Their tunable photoluminescence wavelengths are especially important for next-generation lighting devices (Banerjee & Saparov, 2023). Compared to the extensively studied lead-halide materials, copper-based halides also have the advantage of lower toxicity.

Copper(I) halides reported so far, with both inorganic and organic counter-ions, typically form zero-dimensional or one-dimensional structures, such as Rb_2CuBr_3 (Creason *et al.*, 2020), $(Bmpip)_2Cu_2Br_4$ (where Bmpip = 1-butyl-1-methylpiperidinium; Xu *et al.*, 2022), and PPh_4CuBr_2 (Xu *et al.*, 2022) and 1D-$(Npipz)_2Cu_2I_6$ (where Npipz = 1-butyl-1-methylpiperidinium; Carignan *et al.*, 2024). These compounds have become known as highly efficient blue-light emitters, up-conversion materials, and scintillators with large light yields,

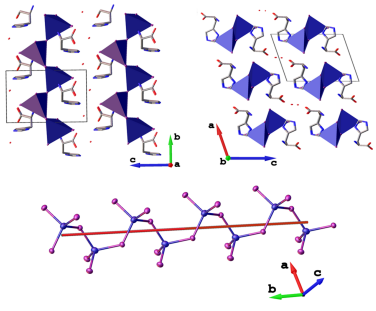

mainly because of efficient recombination pathways involving self-trapped excitons (STE).

Recently, one-dimensional copper(I) halides with the general formula A_2CuX_3 have become more studied. These materials, made up of $[CuX_3]_n^{2n-}$ chains formed through corner-sharing $[CuX_4]$ tetrahedra, exhibit decent photoluminescence quantum yields and often excellent scintillation performance. Although such materials are still relatively rare, these one-dimensional copper(I) halides show halide-tunable luminescence in the lower-wavelength visible range, emitting blue, purple, and cyan light - an attractive feature for lighting and display applications (Carignan *et al.*, 2024; Du *et al.*, 2023; Zhang *et al.*, 2024).

Introducing chirality into these systems could enhance their functionality, enabling polarized light emission in the visible range and expanding their potential for nonlinear optical applications. Chiral α-amino acids, particularly L-histidine, have been shown to act as effective structure-directing agents in the synthesis of chiral metal halides, including hybrid perovskite materials (Sirenko *et al.*, 2024, 2023). L-Histidine is particularly notable because it can adopt two protonation states, existing as either the mono or diprotonated L-histidinium.

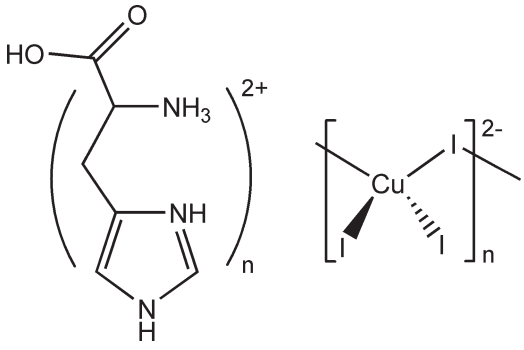

In this paper we report a new chiral low-dimensional copper(I) iodide hybrid material obtained using the reaction between L-histidine and copper(I) iodide in concentrated hydroiodic acid. A detailed structural characterization and a Hirshfeld surface analysis were carried out for the resulting compound, (L-HisH$_2$)CuI$_3$·H$_2$O (**1**).

2. Structural commentary

The title compound crystallizes in the monoclinic space group $P2_1$. The asymmetric unit of **1** contains one L-histidinium cation, one Cu^+ cation, three iodide anions and a co-crystallized water molecule (Fig. 1). Each Cu^+ cation coordinated by four iodide ligands adopts a tetrahedral coordination geometry (Fig. 1). In each $[CuI_4]$ tetrahedron, two iodide atoms bridge neighboring Cu^I centers, while the other two are terminal, interacting only with Cu^I and forming hydrogen bonds with the L-histidinium cations and co-crystallized water molecules (Fig. 1). The Cu—I bond lengths in the $[CuI_4]$ coordination tetrahedra range from 2.62 to 2.72 Å (Table 1), which is similar to values observed in other A_2CuI_3-type compounds reported to date (Zhang *et al.*, 2024; Carignan *et al.*, 2024; Du *et al.*, 2023). The I—Cu—I bond angles in the $[CuI_4]$ tetrahedra range from 106.19 to 113.21°, deviating from the ideal tetrahedral value of ∼109.5° and demonstrating a smaller angle deviation compared to the previously reported compounds (Zhang *et al.*, 2024; Carignan *et al.*, 2024; Du *et al.*, 2023). In **1**, the Cu—I bonds with the terminal iodides (∼2.63 Å) are shorter than those with the bridging μ-iodides (∼2.71 Å), consistent with previously reported A_2CuI_3 compounds (Zhang *et al.*, 2024; Carignan *et al.*, 2024; Du *et al.*, 2023). The Cu—μ-I—Cu bridging angle between adjacent tetrahedra is 125.79 (3)°, notably larger than the ∼108° observed in other A_2CuI_3 compounds (Zhang *et al.*, 2024; Carignan *et al.*, 2024; Du *et al.*, 2023).

Table 1
Selected geometric parameters (Å, °).

I1—Cu1^{i}	2.7063 (13)	I2—Cu1	2.6225 (12)
I1—Cu1	2.7216 (13)	I3—Cu1	2.6433 (11)
Cu1^{i}—I1—Cu1	125.80 (3)	I2—Cu1—I3	106.19 (4)
I1^{ii}—Cu1—I1	109.20 (4)	I3—Cu1—I1^{ii}	110.75 (4)
I2—Cu1—I1	107.70 (4)	I3—Cu1—I1	113.21 (5)
I2—Cu1—I1^{ii}	109.68 (5)		

Symmetry codes: (i) $-x, y-\frac{1}{2}, -z+1$; (ii) $-x, y+\frac{1}{2}, -z+1$.

A convenient way to describe distortions in coordination polyhedra is by using distortion indices. Several indices have been introduced in the literature, particularly for metal–oxygen tetrahedra. Baur proposed the following distortion indices for metal–oxide tetrahedra (Baur, 1970):

$$DI(AX) = \Sigma^4_{i=1} \mid (A-X)_i - \langle A-X \rangle \mid / (4 < A-X >),$$

$$DI(XAX) = \Sigma^6_{i=1} \mid (X-A-X)_i - < X-A-X > \mid / (6 < X-A-X >)$$

and

$$DI(XX) = \Sigma^6_{i=1} \mid (X\cdots X)_i - < X\cdots X > \mid / (6 < X\cdots X >).$$

Here, DI(AX), DI(XX) and DI(XAX) represent the bond-length distortion parameter (BLDP), edge-length distortion parameter (ELDP) and bond-angle distortion parameter

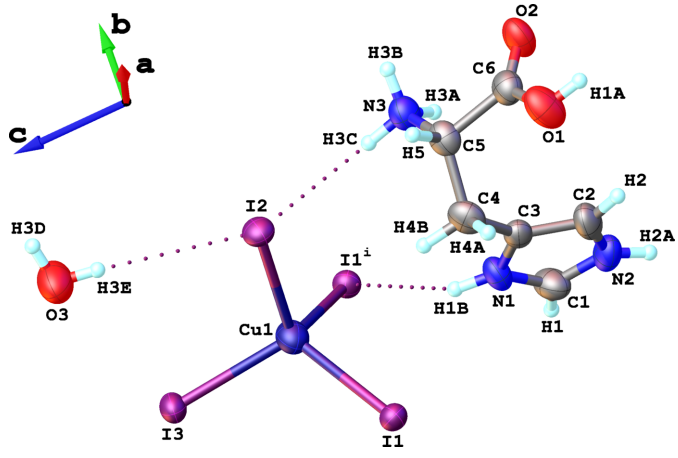

Figure 1
Representation of the building units in the crystal structure of **1**, showing the atom-labeling scheme. Displacement ellipsoids are drawn at the 50% probability level. H atoms are shown as small spheres of arbitrary radius. [Symmetry codes: (i) $-x, \frac{1}{2}+y, 1-z$].

Table 2
Selected octahedral distortion parameters.

	L-HisH$_2$[CuI$_3$]·H$_2$O[a]	1D-(Npipz)$_2$Cu$_2$I$_6$[b]	[1,2-PDA]CuI$_3$[c]	[1,3-PDA]CuI$_3$[d]
DI(AX)	0.0152	0.00941	0.00927	0.02204
DI(XAX)	0.01608	0.04301	0.02587	0.03077
DI(XX)	0.01615	0.03742	0.01557	0.01237
τ_4	0.965	0.937	0.941	0.931
τ_4'	0.957	0.934	0.935	0.914

(*a*) The title compound (**1**); (*b*) Carignan *et al.* (2024); (*c*) Du *et al.* (2023); (*d*) Zhang *et al.* (2024).

(BADP), respectively, which together provide a complete description of the distortion of coordination tetrahedra. Although these indices were originally developed for ionic metal–oxygen systems, they can also be applied to tetrahedra with Cu—I bonds, which have partial covalent character. The calculated values for compound **1** are DI(AX) = 0.0152, DI(XAX) = 0.01608, and DI(XX) = 0.01615 (Table 2). Among A_2CuI_3-type compounds, **1** shows the highest DI(AX) value, whereas its DI(XAX) and DI(XX) values are the lowest reported for this family. Additionally, the parameter τ_4 which was developed for four-coordinated structures, is often used to describe deviations from ideal tetrahedral geometry (Yang *et al.*, 2007). For square planar structures, $\tau_4 = 0$, whereas for tetrahedral structures, $\tau_4 = 1$:

$$\tau_4 = [360^\circ - (\alpha + \beta)] / [360^\circ - 2\theta],$$

where β is the largest and α is the second-largest bond angle ($\beta > \alpha$) in a four-coordinate geometry, and $\theta = \arccos(-1/3) \approx 109.5^\circ$ is the ideal tetrahedral angle.

This parameter was later refined to more effectively distinguish between four-coordinate complexes that have significantly different geometries but similar τ_4 values. The revised parameter, τ_4' (Okuniewski *et al.*, 2015), provides values comparable to τ_4 but offers improved discrimination among the examined structures ($\tau_4' > \tau_4$):

$$\tau_4' = [(\beta - \alpha) / (360^\circ - \theta)] + [(180^\circ - \beta) / (180^\circ - \theta)]$$

(α, β and θ as before). For **1**, τ_4 and τ_4' are 0.965 and 0.957, respectively, indicating a slight distortion of the [CuI$_4$] tetrahedra relative to the ideal geometry ($\tau_4 = \tau_4' = 1$) (Table 2). These values are the highest reported among related one-dimensional copper(I) halides, suggesting that the [CuI$_4$] tetrahedra in **1** are the least distorted within this family (Table 2).

The [CuI$_4$] coordination polyhedra participate in both μ_2-bridging coordination (Cu—μ-I—Cu) and hydrogen bonding with the L-histidinium cations, forming infinite $[CuI_3]_n^{2n-}$ polymeric chains that propagate along the [010] direction (Fig. 2). Interestingly, the $[CuI_3]_n^{2n-}$ chains (point group 2) exhibit left-handed helical chirality, suggesting a structure-directing role of the chiral L-histidinium cations in the formation of these helical chains (Fig. 2*c*). Moreover, the Cu···Cu distance of 4.83 Å between adjacent tetrahedra is the largest reported among compounds featuring one-dimensional chains of corner-sharing [CuI$_4$] tetrahedra (Zhang *et al.*, 2024; Carignan *et al.*, 2024; Du *et al.*, 2023).

3. Supramolecular features

The L-histidinium cations and co-crystallized water molecules interact with the one-dimensional helical chains of corner-sharing [CuI$_4$] tetrahedra through a network of N—H···I and O—H···I hydrogen bonds, along with weak C—H···I

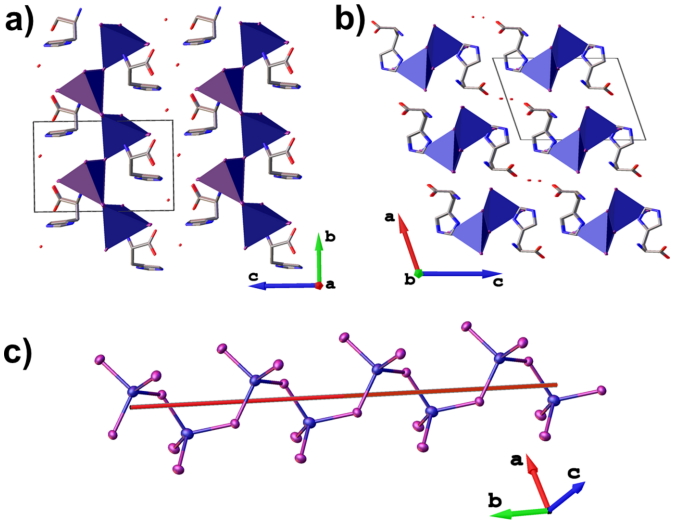

Figure 2
Crystal packing of **1** viewed along (*a*) the [100] and (*b*) the [010] directions, and (*c*) side view of a fragment of the crystal structure showing an inorganic chain with left-handed helical chirality.

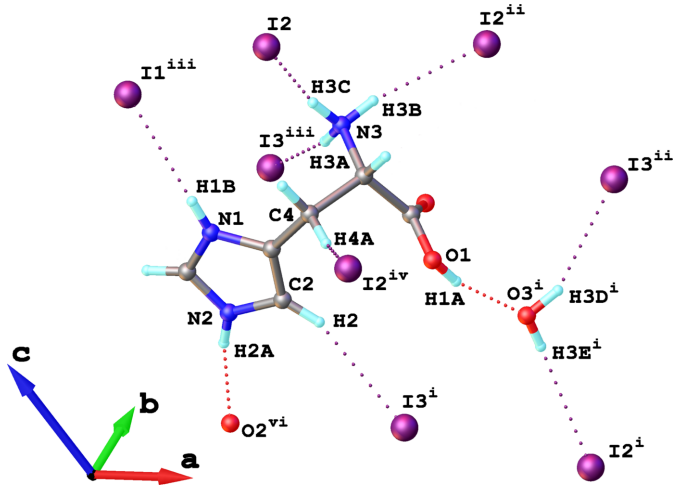

Figure 3
Side views of a fragment of the crystal structure of **1**, illustrating the hydrogen-bonding scheme of the L-histidinium cation (dotted lines). [Symmetry codes: (i) $x, y, -z+1$; (ii) $-x+1, y+\frac{1}{2}, -z+1$; (iii) $-x, y+\frac{1}{2}, -z+1$; (iv) $-x+1, y-\frac{1}{2}, -z+1$; (v) $-x+1, y, z$; (vi) $-x, \frac{1}{2}+y, -z$].

Table 3
Hydrogen-bond geometry (Å, °).

D—H···A	D—H	H···A	D···A	D—H···A
O3—H3D···I3^{iii}	0.86	3.02	3.768 (8)	146
O3—H3E···I2	0.82	3.12	3.938 (7)	177
O1—H1A···O3^{iv}	0.82	1.81	2.605 (10)	162
N3—H3A···I3^{ii}	0.89	2.69	3.571 (8)	169
N3—H3B···I2^{v}	0.89	2.75	3.601 (8)	160
N3—H3C···I2	0.89	2.79	3.596 (7)	152
N1—H1B···I1^{ii}	0.86	2.81	3.516 (7)	141
N2—H2A···O2^{vi}	0.86	1.97	2.804 (9)	163
C4—H4A···I2^{vii}	0.97	2.88	3.716 (9)	146

Symmetry codes: (ii) $-x, y+\frac{1}{2}, -z+1$; (iii) $-x+1, y+\frac{1}{2}, -z+2$; (iv) $x, y, z-1$; (v) $-x+1, y+\frac{1}{2}, -z+1$; (vi) $-x, y-\frac{1}{2}, -z$; (vii) $-x+1, y-\frac{1}{2}, -z+1$.

contacts (Fig. 3, Table 3). In **1**, the L-histidinium cation is doubly protonated at both the imidazolium ring and the amino group, which enables the formation of the A_2CuX_3-type structure. The protonated amino group participates in N—H···I hydrogen bonding with two adjacent $[CuI_3]_n^{2-}$ chains. Specifically, two hydrogen bonds, N3$_{(a)}$—H3$B_{(a)}$···I2^{ii} and N3$_{(a)}$—H3$C_{(a)}$···I2 [subscript (a) denotes the amino group], connect the L-histidinium cation to one chain, while N3$_{(a)}$—H3$A_{(a)}$···I3^{iii} links it to a second chain (Fig. 3). The protonated imidazolium ring contributes to linking neighboring $[CuI_3]_n^{2n-}$ chains *via* N1$_{(i)}$—H1$B_{(i)}$···I1^{iii} hydrogen bonds [where (i) denotes the imidazolium ring] (Table 3, Fig. 3). The carboxyl group of the L-histidinium cation and the co-crystallized water molecules further consolidate the organic—inorganic framework through hydrogen-bonding interactions. In particular, the hydroxyl group of the carboxyl participates in O1$_{(c)}$—H1$A_{(c)}$···O3$_{(w)}{}^{i}$ hydrogen bonding with the co-crystallized water molecules (Fig. 3), where (w) denotes co-crystallized water and (c) denotes the carboxyl group. The co-crystallized water molecule participates in O3$_{(w)}{}^{i}$—H3E^{i}···I2^{i} and O3$_{(w)}{}^{i}$—H3D^{i}···I3^{ii} hydrogen bonding with two inorganic chains (Fig. 3, Table 3). The L-histidinium cations interact with each other through an N2$_{(i)}$—H2$A_{(i)}$···O2$_{(c)}{}^{vi}$ hydrogen bond (Fig. 3), which links the imidazolium N—H group of one cation to the carbonyl oxygen of the carboxyl group of another cation.

Furthermore, the secondary CH_2 group of the aliphatic backbone of L-histidinium also participate in weak C4—H4A···I2^{iv} (Fig. 3) contacts, further reinforcing the cohesion between the organic and inorganic components of **1**. As previously established, C—H···B (where B denotes the hydrogen bond acceptor) hydrogen bonding can be considered when (r C···B) – [$r_{vdW}(B)$ + r C—H] < 1.00 Å, where r C—H is the average C—H bond length, and $r_{vdW}(B)$ is the van der Waals radius of the hydrogen-bond acceptor (Harmon *et al.*, 1992). For the weak C2—H2···I3^{i} contacts (Fig. 3) involving the imidazolium ring, the (r C···B) – [$r_{vdW}(B)$ + r C—H] difference is 0.91 Å with a bond angle of 157°, which lies within the expected range for such interactions. For C4—H4A···I2^{iv} weak contact (Fig. 3) (secondary CH_2 group), the difference is 0.686 Å with a bond angle of 145°, indicating weak hydrogen bonding. Moreover, the imidazolium moiety of L-histidinium participates in an I···π interaction (Fig. 4) with the I3 atom of $[CuI_4]$ unit, with centroid···I3^{i} and centroid···I3^{ii} distances of of 4.056 (4) and 3.697 (4) Å, respectively, and an I3^{i}···centroid···I3^{ii} angle of 155.36 (12)°, which falls within the range previously reported for I···π interactions (Prasanna & Guru Row, 2000). Concave red regions on the Hirshfeld surface mapped with the shape-index function (Fig. 4*b*,*c*) further indicate the presence of I···π interactions in the compound.

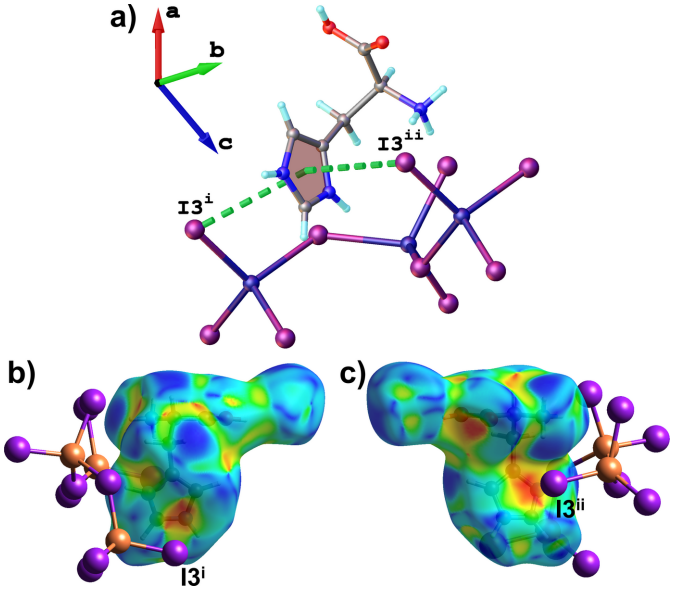

Figure 4
(*a*) Side views of a fragment of the crystal structure of **1**, illustrating I···π interactions (green dashed line). (*b*), (*c*) The Hirshfeld surface mapped with the shape-index function highlights I···π interactions between I3^{i} and I3^{ii} atoms and the imidazolium ring. [Symmetry codes: (i) $-x, y-\frac{1}{2}, 1-z$; (ii) $-x, y+\frac{1}{2}, -z+1$].

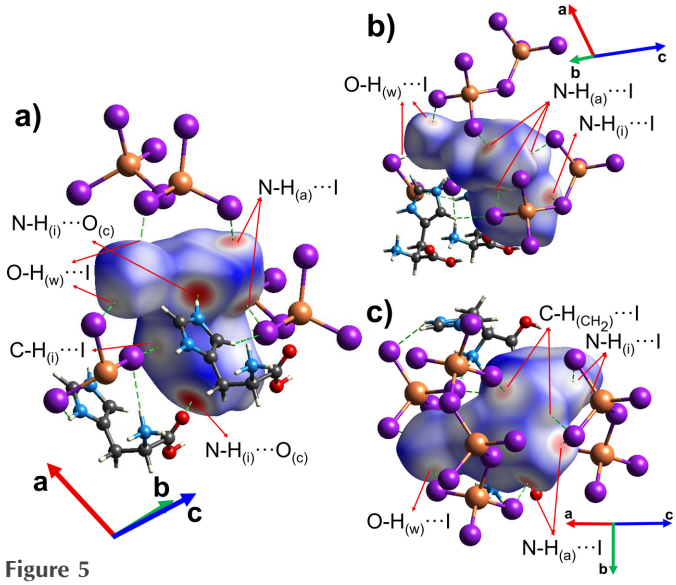

Figure 5
(*a*)–(*c*) Representation of the Hirshfeld surface of the L-histidinium cation in **1** along different crystallographic directions, with the d_{norm} function plotted onto the surface to highlight various interactions. The subscripts indicate different functional groups: (a) = NH_3^+; (c) = COOH; (i) = imidazolium ring; (w) = co-crystallized water molecule; (CH_2) = methylene group.

4. Hirshfeld surface analysis

The Hirshfeld surface and the corresponding two-dimensional fingerprint plots were generated for the fragment containing the L-histidinium cation and the co-crystallized water molecule using *CrystalExplorer 21.5* (Spackman *et al.*, 2021) with standard resolution for the three-dimensional d_{norm} surfaces (Figs. 5 and 6). The red spots on the Hirshfeld surface are attributed to hydrogen bonds and weak C—H···I contacts between this fragment and both the $[CuI_3]_n^{2n-}$ anionic chains and other L-histidinium cations (only hydrogen bonds) (Fig. 5). The associated fingerprint plots (Fig. 6) confirm that hydrogen bonding dominates the crystal packing of **1**. The analysis shows that H···I interactions are predominant (Fig. 6*b*), accounting for approximately 33% of the total Hirshfeld surface. These correspond to N—H···I and O—H···I hydrogen bonds, as well as the weaker C—H···I contacts that link the organic and inorganic components. H···O contacts are the second most significant, contributing approximately 25% (Fig. 6*c*) to the Hirshfeld surface, and arise from O—H···O and N—H···O hydrogen bonds. The contribution of C···I and N···I contacts (less than 5%) to the Hirshfeld surface indicates the presence of I···π interactions (Fig. 6*d* and 6*e*), which further consolidate the crystal packing of **1**.

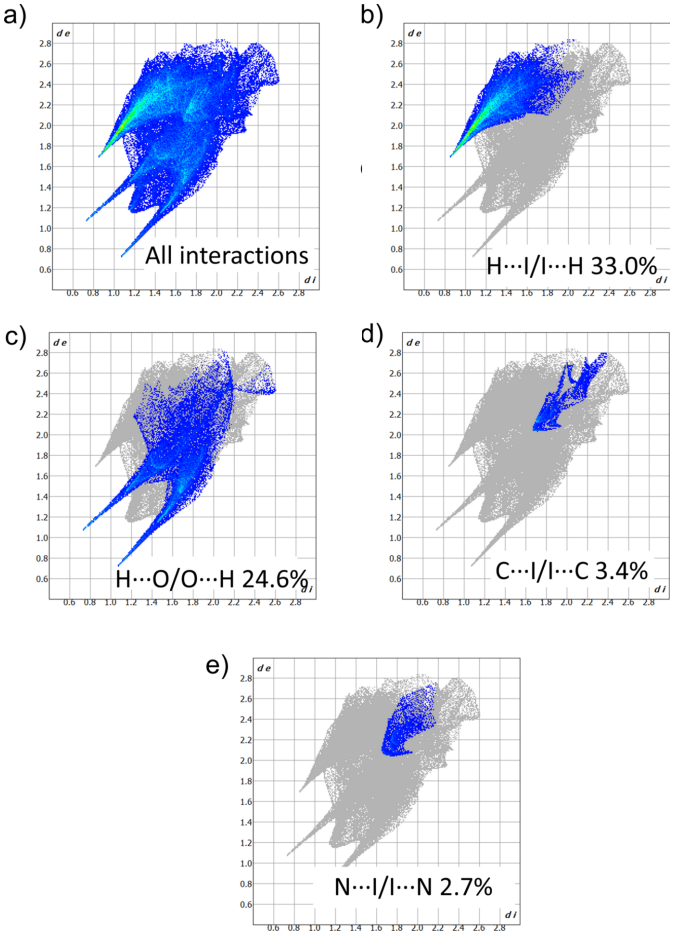

Figure 6
Two-dimensional fingerprint plots from a Hirshfeld surface analysis of **1** showing: (*a*) all contacts; (*b*) H···I/I···H (33.0%); (*c*) H···O/O···H (24.6%); (*d*) C···I/I···C (3.4%); (*e*) N···I/I···N (2.7%).

Table 4
Experimental details.

Crystal data	
Chemical formula	$(C_6H_{11}N_3O_2)[CuI_3]\cdot H_2O$
M_r	619.43
Crystal system, space group	Monoclinic, $P2_1$
Temperature (K)	299
a, b, c (Å)	8.5704 (3), 7.5748 (2), 12.3860 (4)
β (°)	109.113 (3)
V (Å^3)	759.76 (4)
Z	2
Radiation type	Mo $K\alpha$
μ (mm^{-1})	7.53
Crystal size (mm)	0.18 × 0.15 × 0.12
Data collection	
Diffractometer	XtaLAB Synergy, Dualflex, HyPix
Absorption correction	Analytical (*CrysAlis PRO*; Rigaku OD, 2024)
T_{min}, T_{max}	0.398, 0.517
No. of measured, independent and observed [$I > 2\sigma(I)$] reflections	10397, 3728, 3615
R_{int}	0.025
(sin $\theta/\lambda)_{max}$ (Å^{-1})	0.710
Refinement	
$R[F^2 > 2\sigma(F^2)]$, $wR(F^2)$, S	0.029, 0.073, 1.05
No. of reflections	3728
No. of parameters	147
No. of restraints	1
H-atom treatment	H-atom parameters constrained
$\Delta\rho_{max}$, $\Delta\rho_{min}$ (e Å^{-3})	0.98, −0.86
Absolute structure	Flack x determined using 1510 quotients $[(I^+)-(I^-)]/[(I^+)+(I^-)]$ (Parsons *et al.*, 2013)
Absolute structure parameter	−0.03 (4)

Computer programs: *CrysAlis PRO* (Rigaku OD, 2024), *SHELXT2018/2* (Sheldrick, 2015*a*), *SHELXL2019/3* (Sheldrick, 2015*b*) and *OLEX2* (Dolomanov *et al.*, 2009).

5. Database survey

A search of the Cambridge Structure Database (CSD version 6.00, last update August 2025; Groom *et al.*, 2016) revealed 614 structures for the $[CuI_4]$ moiety. Most similar to the title compound, namely complexes containing one-dimensional $[CuI_3]_n^{2n-}$ chains of corner-shared tetrahedra, are *catena*-[1-methylpiperazine-1,4-diium (μ-iodo)diiodocopper] (BOKLEW; Carignan *et al.*, 2024), *catena*-[propane-1,2-diammonium (μ-iodo)bis(iodo)dicopper(I)] (FOSMAF; Zhang *et al.*, 2024), and *catena*-[propane-1,3-bis(ammonium) (μ-iodo)-bis(iodo)copper(I)] (MISJAD; Du *et al.*, 2023).

6. Synthesis and crystallization

L-histidine (20 mg, 0.129 mmol) and copper(I) iodide (25 mg, 0.131 mmol) were dissolved in 600 µL of concentrated HI (57%) and 25 µL of H_3PO_2. The resulting mixture was left to evaporate, and after 2 weeks, colorless, plate-like crystals of the $(L\text{-}HisH_2)CuI_3\cdot H_2O$ compound were obtained. These crystals were placed under crystallographic oil until further single crystal X-ray diffraction measurements.

7. Refinement details

Crystal data, data collection, and structure refinement details are summarized in Table 4. All H atoms were placed geometrically and refined as riding, with C—H = 0.98 Å and U_{iso}(H) = 1.2U_{eq}(C) for ternary CH; C—H = 0.97 Å and U_{iso}(H) = 1.2U_{eq}(C) for secondary CH_2; N—H = 0.86 Å and U_{iso}(H) = 1.2U_{eq}(N) for aromatic NH; C—H = 0.93 Å and U_{iso}(H) = 1.5U_{eq}(C) for aromatic CH groups; O—H = 0.86 Å and U_{iso}(H) = 1.5U_{eq}(O) for water molecules. Amino H atoms were positioned geometrically and allowed to ride on N atoms and rotate around the C—N bond, with N—H = 0.89 Å and U_{iso}(H) = 1.5U_{eq}(N) for NH_3 groups. Carboxylate H atoms were positioned geometrically and allowed to ride on O atoms and rotate around the O—C bond, $O_{(c)}$—H = 0.82 Å (c = carboxylate) and U_{iso}(H) = 1.5U_{eq}(O) for the $O_{(c)}$—H groups of carboxylate.

Acknowledgements

The authors are grateful to the FAIRE programme provided by the Cambridge Crystallographic Data Centre (CCDC) for the opportunity to use the Cambridge Structural Database (CSD) and associated software. VYS acknowledges the II European Chemistry School for Ukrainians.

Funding information

Funding for this research was provided by: Ministry of Education and Science of Ukraine (grant No. 24BF037-01M).

References

Banerjee, D. & Saparov, B. (2023). *Chem. Mater.* **35**, 3364–3385.
Baur, W. H. (1970). *ACA Transactions* **6**, 129–155.
Carignan, G. M., Teat, S. J., Hei, X. & Li, J. (2024). *J. Lumin.* **269**, 120435.
Chen, J., Zhou, K., Li, J., Xu, G., Hei, X. & Li, J. (2025). *Chem. Sci.* **16**, 1106–1114.
Creason, T. D., Yangui, A., Roccanova, R., Strom, A., Du, M. & Saparov, B. (2020). *Adv. Opt. Mater.* **8**, 6–11.
Dolomanov, O. V., Bourhis, L. J., Gildea, R. J., Howard, J. A. K. & Puschmann, H. (2009). *J. Appl. Cryst.* **42**, 339–341.
Du, Y., Ma, L., Yan, Z., Xiao, J., Wang, K., Lin, T., Han, X. & Xia, D. (2023). *Inorg. Chem.* **62**, 11350–11359.
Groom, C. R., Bruno, I. J., Lightfoot, M. P. & Ward, S. C. (2016). *Acta Cryst.* B**72**, 171–179.
Harmon, K. M., De Santis, N. J. & Brandt, D. O. (1992). *J. Mol. Struct.* **265**, 47–57.
Kirakci, K., Fejfarová, K., Martinčík, J., Nikl, M. & Lang, K. (2017). *Inorg. Chem.* **56**, 4609–4614.
Okuniewski, A., Rosiak, D., Chojnacki, J. & Becker, B. (2015). *Polyhedron* **90**, 47–57.
Parsons, S., Flack, H. D. & Wagner, T. (2013). *Acta Cryst.* B**69**, 249–259.
Popy, D. A., Singh, Y., Tratsiak, Y., Cardoza, A. M., Lane, J. M., Stand, L., Zhuravleva, M., Rai, N. & Saparov, B. (2024). *Aggregate* **5**, 1–16.
Prasanna, M. & Guru Row, T. (2000). *Cryst. Eng.* **3**, 135–154.
Rigaku OD (2024). *CrysAlis PRO*. Rigaku Oxford Diffraction, Yarnton, England.
Sheldrick, G. M. (2015*a*). *Acta Cryst.* A**71**, 3–8.
Sheldrick, G. M. (2015*b*). *Acta Cryst.* C**71**, 3–8.
Sirenko, V. Y., Kucheriv, O. I., Fritsky, I. O., Gumienna-Kontecka, E., Dascălu, I.-A., Shova, S. & Gural'skiy, I. A. (2023). *Dalton Trans.* **52**, 10545–10556.
Sirenko, V. Y., Kucheriv, O. I., Shova, S. & Gural'skiy, I. A. (2024). *Mater. Today* **41**, 102452.
Spackman, P. R., Turner, M. J., McKinnon, J. J., Wolff, S. K., Grimwood, D. J., Jayatilaka, D. & Spackman, M. A. (2021). *J. Appl. Cryst.* **54**, 1006–1011.
Xu, T., Li, Y., Nikl, M., Kucerkova, R., Zhou, Z., Chen, J., Sun, Y. Y., Niu, G., Tang, J., Wang, Q., Ren, G. & Wu, Y. (2022). *Appl. Mater. Interfaces* **14**, 14157–14164.
Yang, L., Powell, D. R. & Houser, R. P. (2007). *Dalton Trans.* **9**, 955–964.
Zhang, P., Yan, Z., Li, C., Du, Y., Ma, L., Wang, Z., Lin, T., Zhao, L. & Xiao, J. (2024). *Chem. Eng. J.* **496**, 154106.

supporting information

Acta Cryst. (2025). E**81**, 1158-1163 [https://doi.org/10.1107/S2056989025010023]

Crystal structure and Hirshfeld surface analysis of chiral *catena*-poly[L-histidinediium [[diiodidocuprate(I)]-μ-iodido] monohydrate]

Valerii Y. Sirenko, Valeriia N. Ovdenko, Vadim A. Potaskalov, Mircea-Odin Apostu and Il'ya A. Gural'skiy

Computing details

***catena*-Poly[4-[(2*S*)-2-azaniumyl-2-carboxyethyl]-1*H*-imidazol-3-ium [[diiodidocuprate(I)]-μ-iodido] monohydrate]**

Crystal data

$(C_6H_{11}N_3O_2)[CuI_3]\cdot H_2O$
$M_r = 619.43$
Monoclinic, $P2_1$
$a = 8.5704$ (3) Å
$b = 7.5748$ (2) Å
$c = 12.3860$ (4) Å
$\beta = 109.113$ (3)°
$V = 759.76$ (4) Å^3
$Z = 2$
$F(000) = 564$
$D_x = 2.708$ Mg m^{-3}
Mo $K\alpha$ radiation, $\lambda = 0.71073$ Å
Cell parameters from 8127 reflections
$\theta = 2.6$–$30.0°$
$\mu = 7.53$ mm^{-1}
$T = 299$ K
Plate, clear intense colourless
0.18 × 0.15 × 0.12 mm

Data collection

XtaLAB Synergy, Dualflex, HyPix diffractometer
Radiation source: micro-focus sealed X-ray tube, PhotonJet (Mo) X-ray Source
Mirror monochromator
Detector resolution: 10.0000 pixels mm^{-1}
ω scans
Absorption correction: analytical (CrysAlisPro; Rigaku OD, 2024)
$T_{min} = 0.398$, $T_{max} = 0.517$
10397 measured reflections
3728 independent reflections
3615 reflections with $I > 2\sigma(I)$
$R_{int} = 0.025$
$\theta_{max} = 30.3°$, $\theta_{min} = 2.5°$
$h = -11\rightarrow11$
$k = -10\rightarrow10$
$l = -15\rightarrow17$

Refinement

Refinement on F^2
Least-squares matrix: full
$R[F^2 > 2\sigma(F^2)] = 0.029$
$wR(F^2) = 0.073$
$S = 1.05$
3728 reflections
147 parameters
1 restraint
Primary atom site location: dual
Hydrogen site location: mixed
H-atom parameters constrained
$w = 1/[\sigma^2(F_o^2) + (0.0449P)^2 + 0.2675P]$ where $P = (F_o^2 + 2F_c^2)/3$
$(\Delta/\sigma)_{max} < 0.001$
$\Delta\rho_{max} = 0.98$ e Å^{-3}
$\Delta\rho_{min} = -0.86$ e Å^{-3}
Absolute structure: Flack *x* determined using 1510 quotients $[(I^+)-(I^-)]/[(I^+)+(I^-)]$ (Parsons *et al.*, 2013)
Absolute structure parameter: −0.03 (4)

Special details

Geometry. All esds (except the esd in the dihedral angle between two l.s. planes) are estimated using the full covariance matrix. The cell esds are taken into account individually in the estimation of esds in distances, angles and torsion angles; correlations between esds in cell parameters are only used when they are defined by crystal symmetry. An approximate (isotropic) treatment of cell esds is used for estimating esds involving l.s. planes.

Fractional atomic coordinates and isotropic or equivalent isotropic displacement parameters (Å²)

	x	*y*	*z*	U_{iso}*/U_{eq}
I1	0.13680 (5)	0.06749 (6)	0.50811 (4)	0.03160 (12)
I2	0.40061 (6)	0.55289 (7)	0.62736 (4)	0.03880 (13)
I3	0.13407 (6)	0.34038 (8)	0.82833 (4)	0.03910 (14)
Cu1	0.13059 (14)	0.37960 (17)	0.61550 (9)	0.0467 (3)
C1	−0.1623 (11)	0.3476 (15)	0.1876 (8)	0.049 (2)
H1	−0.265910	0.333504	0.195383	0.059*
C5	0.3636 (9)	0.5864 (13)	0.3020 (6)	0.0395 (17)
H5	0.477608	0.580101	0.354083	0.047*
C4	0.2814 (11)	0.4064 (12)	0.3052 (8)	0.045 (2)
H4A	0.346960	0.315430	0.285442	0.054*
H4B	0.284618	0.384334	0.383101	0.054*
C3	0.1048 (10)	0.3873 (10)	0.2276 (6)	0.0340 (15)
C2	0.0371 (12)	0.3698 (14)	0.1142 (7)	0.047 (2)
H2	0.092239	0.372943	0.060802	0.057*
O3	0.5032 (10)	0.6129 (13)	0.9593 (6)	0.071 (2)
H3D	0.580076	0.691853	0.978808	0.107*
H3E	0.481288	0.605276	0.889629	0.107*
O2	0.3119 (9)	0.7716 (9)	0.1368 (5)	0.0524 (16)
O1	0.4420 (10)	0.5140 (11)	0.1428 (6)	0.0608 (19)
H1A	0.439416	0.541704	0.078238	0.091*
N3	0.2782 (10)	0.7316 (10)	0.3429 (6)	0.0433 (16)
H3A	0.177322	0.746996	0.293110	0.065*
H3B	0.335656	0.831167	0.349050	0.065*
H3C	0.270935	0.702959	0.410742	0.065*
C6	0.3693 (10)	0.6362 (13)	0.1839 (7)	0.0416 (18)
N1	−0.0242 (9)	0.3721 (10)	0.2707 (5)	0.0410 (15)
H1B	−0.014808	0.377986	0.341854	0.049*
N2	−0.1306 (9)	0.3461 (11)	0.0917 (5)	0.0479 (17)
H2A	−0.202496	0.332496	0.024939	0.057*

Atomic displacement parameters (Å²)

	U^{11}	U^{22}	U^{33}	U^{12}	U^{13}	U^{23}
I1	0.0338 (2)	0.0288 (2)	0.0311 (2)	−0.00231 (19)	0.00916 (16)	−0.00163 (18)
I2	0.0332 (2)	0.0415 (3)	0.0409 (3)	−0.0090 (2)	0.01095 (18)	−0.0002 (2)
I3	0.0453 (3)	0.0436 (3)	0.0279 (2)	−0.0090 (2)	0.01119 (18)	−0.0014 (2)
Cu1	0.0450 (6)	0.0545 (6)	0.0418 (5)	−0.0078 (5)	0.0160 (4)	0.0006 (5)
C1	0.044 (4)	0.053 (5)	0.050 (5)	−0.007 (4)	0.012 (4)	0.009 (5)
C5	0.029 (3)	0.050 (5)	0.037 (4)	0.008 (3)	0.007 (3)	0.005 (4)

C4	0.042 (4)	0.044 (5)	0.048 (5)	0.013 (3)	0.013 (4)	0.014 (4)
C3	0.041 (4)	0.027 (3)	0.032 (4)	0.003 (3)	0.010 (3)	0.001 (3)
C2	0.063 (6)	0.049 (5)	0.032 (4)	0.006 (4)	0.019 (4)	−0.002 (4)
O3	0.078 (5)	0.088 (6)	0.051 (4)	−0.022 (4)	0.026 (4)	−0.006 (4)
O2	0.064 (4)	0.056 (4)	0.036 (3)	0.015 (3)	0.013 (3)	0.009 (3)
O1	0.065 (4)	0.072 (5)	0.055 (4)	0.019 (4)	0.033 (3)	0.012 (3)
N3	0.047 (4)	0.046 (4)	0.038 (4)	0.004 (3)	0.015 (3)	0.002 (3)
C6	0.036 (4)	0.049 (5)	0.036 (4)	−0.001 (3)	0.006 (3)	0.001 (3)
N1	0.049 (4)	0.046 (4)	0.029 (3)	0.008 (3)	0.014 (3)	0.006 (3)
N2	0.054 (4)	0.044 (4)	0.035 (3)	0.001 (4)	−0.001 (3)	−0.003 (3)

Geometric parameters (Å, º)

I1—Cu1^{i}	2.7063 (13)	C3—C2	1.339 (11)
I1—Cu1	2.7216 (13)	C3—N1	1.381 (10)
I2—Cu1	2.6225 (12)	C2—H2	0.9300
I3—Cu1	2.6433 (11)	C2—N2	1.383 (12)
C1—H1	0.9300	O3—H3D	0.8634
C1—N1	1.303 (11)	O3—H3E	0.8224
C1—N2	1.303 (11)	O2—C6	1.202 (12)
C5—H5	0.9800	O1—H1A	0.8200
C5—C4	1.542 (13)	O1—C6	1.308 (12)
C5—N3	1.498 (11)	N3—H3A	0.8900
C5—C6	1.527 (11)	N3—H3B	0.8900
C4—H4A	0.9700	N3—H3C	0.8900
C4—H4B	0.9700	N1—H1B	0.8600
C4—C3	1.511 (12)	N2—H2A	0.8600
Cu1^{i}—I1—Cu1	125.80 (3)	C2—C3—N1	105.7 (7)
I1^{ii}—Cu1—I1	109.20 (4)	N1—C3—C4	121.6 (7)
I2—Cu1—I1	107.70 (4)	C3—C2—H2	126.6
I2—Cu1—I1^{ii}	109.68 (5)	C3—C2—N2	106.8 (7)
I2—Cu1—I3	106.19 (4)	N2—C2—H2	126.6
I3—Cu1—I1^{ii}	110.75 (4)	H3D—O3—H3E	103.6
I3—Cu1—I1	113.21 (5)	C6—O1—H1A	109.5
N1—C1—H1	125.8	C5—N3—H3A	109.5
N2—C1—H1	125.8	C5—N3—H3B	109.5
N2—C1—N1	108.3 (8)	C5—N3—H3C	109.5
C4—C5—H5	107.8	H3A—N3—H3B	109.5
N3—C5—H5	107.8	H3A—N3—H3C	109.5
N3—C5—C4	111.2 (7)	H3B—N3—H3C	109.5
N3—C5—C6	108.4 (7)	O2—C6—C5	122.6 (8)
C6—C5—H5	107.8	O2—C6—O1	125.9 (8)
C6—C5—C4	113.7 (7)	O1—C6—C5	111.5 (8)
C5—C4—H4A	108.3	C1—N1—C3	110.0 (7)
C5—C4—H4B	108.3	C1—N1—H1B	125.0
H4A—C4—H4B	107.4	C3—N1—H1B	125.0
C3—C4—C5	116.0 (7)	C1—N2—C2	109.2 (7)

C3—C4—H4A	108.3	C1—N2—H2A	125.4
C3—C4—H4B	108.3	C2—N2—H2A	125.4
C2—C3—C4	132.6 (8)		
C5—C4—C3—C2	73.1 (12)	N3—C5—C4—C3	63.6 (9)
C5—C4—C3—N1	−111.8 (9)	N3—C5—C6—O2	−0.1 (11)
C4—C5—C6—O2	124.1 (9)	N3—C5—C6—O1	−179.7 (8)
C4—C5—C6—O1	−55.5 (10)	C6—C5—C4—C3	−59.0 (10)
C4—C3—C2—N2	176.1 (8)	N1—C1—N2—C2	0.4 (13)
C4—C3—N1—C1	−176.5 (8)	N1—C3—C2—N2	0.5 (10)
C3—C2—N2—C1	−0.6 (12)	N2—C1—N1—C3	−0.1 (12)
C2—C3—N1—C1	−0.3 (10)		

Symmetry codes: (i) −*x*, *y*−1/2, −*z*+1; (ii) −*x*, *y*+1/2, −*z*+1.

Hydrogen-bond geometry (Å, º)

D—H···*A*	*D*—H	H···*A*	*D*···*A*	*D*—H···*A*
O3—H3*D*···I3^{iii}	0.86	3.02	3.768 (8)	146
O3—H3*E*···I2	0.82	3.12	3.938 (7)	177
O1—H1*A*···O3^{iv}	0.82	1.81	2.605 (10)	162
N3—H3*A*···I3^{ii}	0.89	2.69	3.571 (8)	169
N3—H3*B*···I2^{v}	0.89	2.75	3.601 (8)	160
N3—H3*C*···I2	0.89	2.79	3.596 (7)	152
N1—H1*B*···I1^{ii}	0.86	2.81	3.516 (7)	141
N2—H2*A*···O2^{vi}	0.86	1.97	2.804 (9)	163
C4—H4*A*···I2^{vii}	0.97	2.88	3.716 (9)	146

Symmetry codes: (ii) −*x*, *y*+1/2, −*z*+1; (iii) −*x*+1, *y*+1/2, −*z*+2; (iv) *x*, *y*, *z*−1; (v) −*x*+1, *y*+1/2, −*z*+1; (vi) −*x*, *y*−1/2, −*z*; (vii) −*x*+1, *y*−1/2, −*z*+1.